J. Fluid Mech. (2008), *vol.* 614, *pp.* 67–86.
doi:10.1017/S0022112008003194 Printed in the United Kingdom

Physical interpretation of spiralling-columnar convection in a rapidly rotating annulus with radial propagation properties of Rossby waves

SHIN-ICHI TAKEHIRO

Research Institute for Mathematical Sciences, Kyoto University, Kyoto, Japan
takepiro@gfd-dennou.org

(Received 21 January 2008 and in revised form 3 July 2008)

To aid the physical understanding of spiralling-columnar convection emerging in rapidly rotating spheres and spherical shells, two-dimensional thermal convection in a rapidly rotating annulus is investigated through the radial propagation properties of topographic Rossby waves. Two kinds of the boundaries containing the fluid in the axial direction are considered: a convex type modelling a spherical geometry and a concave type for comparison. The linear stability of a basic state with no motion and uniformly unstable stratification is examined and spirally elongated structures of critical convection are obtained for small Prandtl numbers. An analysis of the energy budget shows that a part of the kinetic energy generated in the region with slightly inclined boundaries is dynamically transferred and dissipates through viscosity in the region with strongly inclined boundaries. This indicates that the Rossby waves propagate from the region with slightly inclined boundaries to the region with strongly inclined boundaries. It is presented that the appearance of a spiral structure corresponds to an increase of the local radial wavenumber of the Rossby waves propagating in the radial direction. The flow patterns obtained using the dispersion relation of the Rossby waves coincide with those of the tailing part of the spiral structure obtained numerically. As the Prandtl number increases, the Rossby waves barely propagate because of strong viscous dissipation, and the flow pattern is localized in the region with slightly inclined boundaries. For convex boundaries with unstable stratification concentrating near the outer boundary and concave boundaries with unstable stratification confined near the inner boundary, the flow patterns tilt in the direction inverse to the case of uniform unstable stratification. The tilting direction of the flow pattern is not determined by the curvature of the boundaries considered but instead by the radial propagation direction of the Rossby waves excited by thermal convection.

1. Introduction

Thermal convection in rotating spheres and spherical shells has been investigated vigorously over the last 40 years for application to the atmospheres of the Sun and Jovian planets and the fluid cores of the planets. A pioneering study of thermal convection in rapidly rotating spheres and spherical shells, performed by Busse (1970), obtained the structure of critical thermal convection in a rapidly rotating sphere using an asymptotic expansion method. The study showed that critical convection is strongly governed by the Taylor–Proudman theorem and that two-dimensional vortices uniform along the rotating axis emerge locally in the middle of a sphere. However, recent numerical calculations have shown that the fluid motion of the

critical state is not necessarily localized (Zhang & Busse 1987; Zhang 1992). When the Prandtl number is large, Taylor-column-type convection similar to the Busse solution occurs locally (columnar convection), whereas as the Prandtl number decreases, convective vortices expand radially and a spiral structure tilting outward in the prograde direction emerges as the critical state (spiralling-columnar convection). A mathematical description of the spiral structure of the critical convection is formulated by improving the Busse asymptotic theory (Yano 1992; Jones, Soward & Mussa 2000; Dormy *et al.* 2003).

An important characteristic of spiral structures is the tilting direction of the convective vortices. Flow patterns tilting outward in the prograde direction are accompanied by angular momentum transport in the radial direction through Reynolds stress, producing a super-rotation state at the outer boundary of the equatorial region. It is considered that this mechanism dominates the generation of the equatorial super-rotation states observed at the surface of the sun and in the Jovian atmospheres (Busse 1983*a*, *b*; Takehiro & Hayashi 1999; Aurnou & Olson 2001; Christensen 2001). The tilting direction of a flow pattern is considered to be determined by the curvature of the boundaries in the direction of the rotating axis (Busse 1983*a*, *b*, 2002). It was shown by asymptotic expansion that a flow pattern tilts outward in the prograde direction when the boundaries are convex, whereas when the boundaries are concave, it tilts inward in the prograde direction.

As described earlier, mathematical descriptions of the critical states of thermal convection in rotating spheres and spherical shells have been successful so far. However, mathematical descriptions alone are not always sufficient to understand the characteristics of a phenomenon. Satisfactory physical explanations of why a spiral structure emerges as the critical state at low Prandtl numbers or why the curvature of the boundaries is related to the tilting direction of the flow pattern have not yet been proposed. For example, it is often stated that the reason for the outward-prograde tilting of the cell is because the propagation speed in the longitudinal direction of the convective flow pattern is higher in the outer region than in the inner region (Busse 2002; Vasavada & Showman 2005). This explanation is appropriate in the case in which the inner and outer parts of the convection travel separately at their own speeds (Schnaubelt & Busse 1992). However, it is an unsatisfactory explanation of spiralling-columnar convection, since a spiral structure, which emerges as a critical mode of the linearized governing equations, propagates at the same speed everywhere.

This paper attempts to physically interpret the properties of spiralling-columnar convection. In order to achieve an intuitive understanding of the phenomenon, a three-dimensional spherical system is not considered; rather, a model of two-dimensional convection in a rotating annulus with inclined boundaries binding the fluid in the axial direction is proposed. This model can extract the dynamical essentials of three-dimensional convection in rapidly rotating spheres and spherical shells (e.g. Busse & Hood 1982; Busse 1986; Busse & Or 1986; Or & Busse 1987; Lin 1990; Schnaubelt & Busse 1992; Takehiro *et al.* 2002; Plaut & Busse 2005). When the rotation rate of the system is large, columnar fluid motion uniform along the rotating axis becomes predominant according to the Taylor–Proudman theorem. The model incorporates the effect of tilting surfaces binding the fluid in the axial direction, i.e. the topographic β effect, with two-dimensional fluid motion.

'Topographic Rossby waves' describe typical fluid motion governed by the topographic β effect. These waves occur through the expansion and contraction of vortex columns by their radial displacement and the inclination of the boundaries binding the fluid in the axial direction. In this paper, a physical understanding of

spiralling-columnar convection is attempted by relating its characteristics with the radial propagation properties of Rossby waves. As a result of this comparison, we show that the outward-prograde tilting pattern is not caused by a phase speed larger in the outer region than in the inner region but by an increase of the radial wavenumber in the outer region due to conservation of the phase speed. The comparison with the Rossby waves will help explain hydrodynamic structures, such as the excitation region of convective motion and the geometry of propagation and dissipation of the Rossby waves.

It should be noted that the Rossby waves discussed here are different from the 'thermal Rossby waves' denoted in the studies so far (e.g. Busse 1986). The thermal Rossby waves refer to the entire structure of longitudinally propagating convective motion affected by the thermal effects, while the traditional purely dynamic Rossby waves are used here. The energy budget analyses presented next will show that the tailing part of the spiralling convection is not dominated by the thermal effects but is governed by the dynamical transfer of kinetic energy and viscous dissipation. Therefore, the tailing part of the spiral structure can be modelled only by the dynamic factors without the thermal effects such as buoyancy and thermal diffusion.

Section 2 describes the mathematical formulation of the rapidly rotating annulus model, and in § 3 a linear stability analysis is performed. On investigating the energy budget of the obtained spiralling convection, it is observed that the kinetic energy produced in the region with weak topographic β effect is dynamically transferred to the region with strong topographic β effect and dissipated by viscosity. On the basis of this picture, the radial propagation characteristics of the Rossby waves are examined, and it is shown that the obtained spiral structure of critical convection can be explained by an increase of a local radial wavenumber of the Rossby waves propagating in the radial direction. We also present the special case in which the tilting direction of the flow pattern becomes inverse to that expected from the curvature of the boundaries and propose that the direction of tilt is determined by the direction of propagation of the Rossby waves excited by thermal convection. Section 4 summarizes our results.

2. Model

Let us consider a Boussinesq fluid filling an annular region bound by equatorially symmetric spherical boundaries cut from a self-gravitating spherical shell, as shown in figure 1. We assume that the annulus rotates rapidly with a rotation rate Ω and that the fluid motion is two-dimensional and uniform in the direction of the rotating axis in order to satisfy the Taylor–Proudman theorem. We introduce the x coordinate in the retrograde azimuthal direction, the y coordinate in the radial direction and the z coordinate in the direction of the rotating axis. Gravity operates in the inward radial direction. The fluid is uniformly warmed at the inner boundary and cooled at the outer boundary. The governing equations are the equation of the z component of the vorticity and the equation of the temperature. Disturbances from the conductive static state are considered and the linearized equations are as follows:

$$\frac{\partial}{\partial t}\nabla^2\psi + P\eta(y)\frac{\partial\psi}{\partial x} = PR\frac{\partial\theta}{\partial x} + P\nabla^2\nabla^2\psi, \tag{2.1}$$

$$\frac{\partial\theta}{\partial t} + \frac{\mathrm{d}\Theta}{\mathrm{d}y}\frac{\partial\psi}{\partial x} = \nabla^2\theta. \tag{2.2}$$

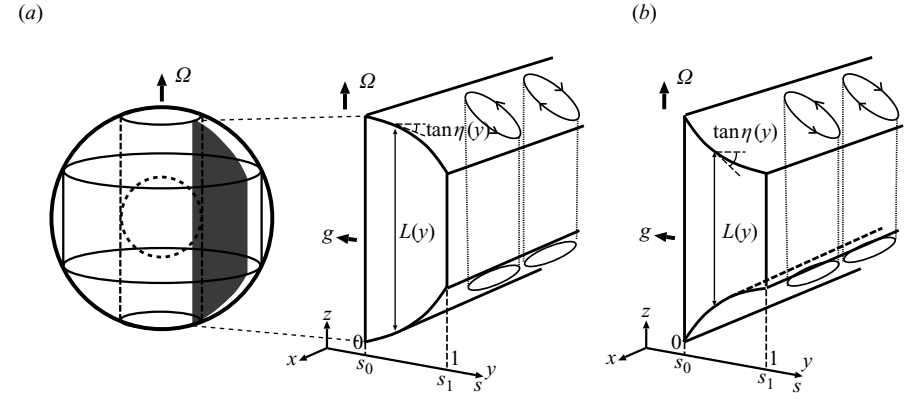

FIGURE 1. Geometry of the system considered: (*a*) case with spherical convex boundaries and (*b*) case with concave boundaries.

The system is non-dimensionalized by using the radial width of the annulus d as the length scale and the thermal diffusive time d^2/κ as the time scale, where κ is the thermal diffusivity; $\psi(x, y, t)$ and $\theta(x, y, t)$ are the stream function and temperature disturbance, respectively; and $\Theta(y)$ is the temperature distribution of the basic state. The term $\nabla^2 = \partial_{xx} + \partial_{yy}$ denotes the two-dimensional Laplacian operator. The non-dimensional parameters $P = \nu/\kappa$ and $R = \alpha g \Delta T d^3/(\kappa\nu)$ are the Prandtl number and the Rayleigh number, respectively, where ν is the kinematic viscosity, α is the coefficient of thermal expansion, g is the gravitational acceleration and ΔT is the temperature difference between the inner and outer boundaries. The boundary condition in the x direction is cyclic and in the y direction is free-slip with fixed temperature:

$$\psi = \frac{\partial^2 \psi}{\partial y^2} = \theta = 0 \quad \text{at} \quad y = 0, 1. \tag{2.3}$$

The coefficient $\eta(y)$ represents the topographic β effect originating from the inclination of the boundaries in the direction of the rotating axis. In studies conducted to date, this coefficient has been assumed to be constant (Busse 1986; Busse & Or 1986; Lin 1990; Takehiro *et al.* 2002) or a linear equation of y, which means that the curvature of the boundaries is constant (e.g. Busse & Hood 1982; Or & Busse 1987; Schnaubelt & Busse 1992; Plaut & Busse 2005). Here it is assumed that the coefficient varies radially, to compare the case with convex boundaries, which model the outer spherical geometry, against the case with concave boundaries. When the variation of the length of the domain in the direction of the rotation axis L is small and the inclination of the boundaries is constant, the coefficient becomes $4\eta_0 d/(LE)$, where η_0 is the inclination of the boundaries and $E = \nu/(\Omega d^2)$ is the Ekman number (Busse 1986). By evaluating this formula at each radial point, it is possible to extend it to the varying inclination cases. When the boundary is expressed as $z = f(s)$, $\eta(y) = -2f'(s)/[f(s)E]$ is obtained, where $s = s(y)$ is the distance from the rotation axis and is associated with y as $s(y) = s_0 + (s_1 - s_0)y$ (see figure 1). When the outer boundary is a sphere of radius r_o, the boundary is expressed as $z = \sqrt{r_o^2 - s(y)^2}$. This gives

$$\eta(y) = \frac{2s(y)}{E\left[r_o^2 - s(y)^2\right]}, \quad s(y) = s_0 + (s_1 - s_0)y. \tag{2.4}$$

In the following section, the parameters are fixed as $r_o = 1.0$, $s_0 = 0.4$, and $s_1 = 0.9$.

For concave boundaries, $z = 1/s(y)$. In this case, the coefficient of the topographic β effect becomes

$$\eta(y) = \frac{2}{Es(y)}, \quad s(y) = s_0 + (s_1 - s_0)y. \tag{2.5}$$

In the following section, the parameters are fixed as $s_0 = 0.05$ and $s_1 = 0.55$.

To obtain the critical state of thermal convection, (2.1) and (2.2) are solved in the following form:

$$\psi(x, y, t) = \tilde{\psi}(y)\exp(\mathrm{i}kx + \sigma t), \quad \theta(x, y, t) = \tilde{\theta}(y)\exp(\mathrm{i}kx + \sigma t). \tag{2.6}$$

This gives

$$\sigma\left(\frac{\mathrm{d}^2}{\mathrm{d}y^2} - k^2\right)\tilde{\psi} + \mathrm{i}kP\eta(y)\tilde{\psi} = \mathrm{i}kPR\tilde{\theta} + P\left(\frac{\mathrm{d}^2}{\mathrm{d}y^2} - k^2\right)^2\tilde{\psi}, \tag{2.7}$$

$$\sigma\tilde{\theta} + \mathrm{i}k\frac{\mathrm{d}\Theta(y)}{\mathrm{d}y}\tilde{\psi} = \left(\frac{\mathrm{d}^2}{\mathrm{d}y^2} - k^2\right)\tilde{\theta}, \tag{2.8}$$

$$\tilde{\psi} = \frac{\mathrm{d}^2\tilde{\psi}}{\mathrm{d}y^2} = \tilde{\theta} = 0 \quad \text{at} \quad y = 0, 1. \tag{2.9}$$

From (2.7), (2.8) and (2.9), it can be seen that the even-order derivatives of $\tilde{\psi}$ and $\tilde{\theta}$ become 0 at $y = 0$ and 1. We obtain the coefficient matrix by expanding $\tilde{\psi}$ and $\tilde{\theta}$ in the y direction with a sin series satisfying the boundary conditions. For each given Prandtl number, the critical state is determined by solving the eigenvalue problem iteratively. The sin series in the y direction is calculated up to the 85th order in §§ 3.1 and 3.2 and the 343rd order in § 3.3. We set the region size in the x direction as 8 and the wavenumbers in the x direction are chosen as $k = (\pi/4)\cdot n$, $n = 1, 2, \ldots$. The Ekman number is fixed to $E = 1.0 \times 10^{-4}$ for all cases.

3. Results

3.1. *Spherical convex boundaries*

Figure 2 shows structures of critical convection for spherical convex boundaries and a uniform basic temperature gradient $\mathrm{d}\Theta/\mathrm{d}y = -1$ for various values of the Prandtl number. The obtained critical states have characteristics similar to those of rapidly rotating spheres and spherical shells. As seen in the distributions of the stream function, radially narrow vortex columns emerge when the Prandtl number is large, while they extend spirally as the Prandtl number decreases. The direction of the tilting is in the positive y and negative x directions (outward in the prograde direction) for all cases. The tilting direction of the flow pattern coincides with the results of an asymptotic expansion with a small parameter of the curvature of the boundaries (Busse 1983*a*, *b*, 2002). The radial extent of the spiral structure of the temperature field is smaller than that of the stream function especially in the cases of small Prandtl numbers.

In order to explain the flow patterns of the critical convection in figure 2, the kinetic and thermal energy budgets are investigated. The equation of kinetic energy is obtained by multiplying ψ by (2.1). Averaging it over one wavelength in the x

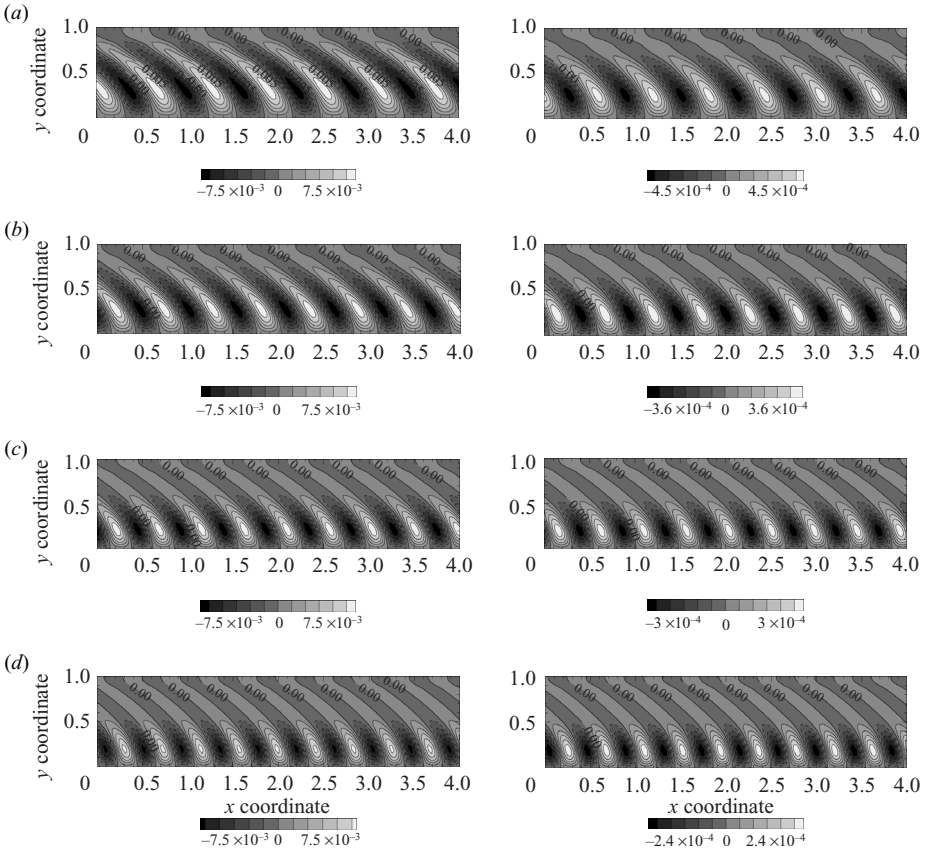

FIGURE 2. Structures of critical convection for spherical convex boundaries and uniform basic temperature gradient $\mathrm{d}\Theta/\mathrm{d}y = -1$ for various values of the Prandtl number: (*a*) $P = 0.1$, (*b*) $P = 0.2$, (*c*) $P = 0.5$ and (*d*) $P = 1.0$. The left and right panels show the stream function and temperature disturbance, respectively.

direction gives

$$\frac{\partial}{\partial t}\left[\frac{1}{2}\overline{|\nabla\psi|^2}\right] = -\frac{\partial}{\partial y}\left(-\overline{\psi\frac{\partial^2\psi}{\partial y\partial t}}\right) - \frac{\partial}{\partial y}\left(P\overline{\psi\frac{\partial\nabla^2\psi}{\partial y}} - P\overline{\frac{\partial\psi}{\partial y}\nabla^2\psi}\right) + PR\theta\overline{\frac{\partial\psi}{\partial x}} - P\overline{(\nabla^2\psi)^2}, \quad (3.1)$$

where the overline denotes the average over one wavelength in the x direction. The left-hand side is the time variation of the kinetic energy, and is equal to zero for the critical state. The third term on the right-hand side is the generation of kinetic energy by the buoyancy force. The fourth term is viscous dissipation. The second term is the convergence of the kinetic energy flux by the viscosity. The first term denotes the energy flux convergence by the dynamic effect; when the thermal and viscous effects are negligible, this term denotes the energy flux convergence by the Rossby waves (Pedlosky 1987). By assuming a plane-wave-type solution, the kinetic energy is observed to be transported with the group velocity of the Rossby waves.

The equation of thermal energy is obtained by multiplying θ by (2.2) and averaging it over one wavelength in the x direction:

$$\frac{\partial}{\partial t}\left[\frac{1}{2}\overline{\theta^2}\right] = -\frac{\mathrm{d}\Theta}{\mathrm{d}y}\overline{\theta\frac{\partial\psi}{\partial x}} - \frac{\partial}{\partial y}\left(-\overline{\theta\frac{\partial\theta}{\partial y}}\right) - \overline{|\nabla\theta|^2}. \tag{3.2}$$

The left-hand side is the time variation of the thermal energy and is equal to zero for the critical state. The first term on the right-hand side is the generation of thermal energy by the vertical fluid motion. The third term is dissipation by thermal diffusivity. The second term is the convergence of the thermal energy flux by diffusivity.

Figure 3 plots each term of the right-hand sides of (3.1) and (3.2) for the critical convection. When the Prandtl number is large, kinetic energy generated in the inner-half region is dissipated by viscosity in the same region. Thermal energy is also generated and dissipated in the inner-half region. As the Prandtl number decreases, the region of viscous dissipation extends outward, whereas the generation of kinetic and thermal energies and the dissipation of thermal energy remain inside the inner-half region. At the same time, the ratio of dynamic-energy flux convergence by the Rossby waves increases. The convergence is negative in the inner region and positive in the outer region, which means that the kinetic energy generated in the inner region is transferred to the outer region. This suggests outward propagation of the Rossby waves excited in the inner region. A part of the kinetic energy generated in the inner region is transferred by the Rossby waves and dissipated in the outer region.

From figure 3 it can be observed that the dynamic factors dominate the energy budget in the outer-half region and the thermal factors become less important as the Prandtl number is decreased. Therefore, in order to explain the flow patterns in the outer region of the critical convection in figure 2, let us investigate (2.1) by neglecting the thermal effect. Moreover, since the Prandtl number is small, the viscous effect is assumed to be negligible for simplicity. Equation (2.1) becomes

$$\frac{\partial}{\partial t}\nabla^2\psi + P\eta(y)\frac{\partial\psi}{\partial x} = 0. \tag{3.3}$$

This equation is the linearized conservation of potential vorticity, and its solution is called the topographic Rossby waves. We require a plane-wave-type solution of (3.3) with a slowly varying amplitude:

$$\psi(x, y, t) = \sum_{n=0}^{\infty} \varepsilon^n \hat{\psi}_n(X, Y, T)\exp[\mathrm{i}\phi(X, Y, T)/\varepsilon], \tag{3.4}$$

where the coordinates

$$X = \varepsilon x, \quad Y = \varepsilon y, \quad T = \varepsilon t \tag{3.5}$$

express the fact that the field is slowly varying. We assume that the coefficient of the topographic β effect is also slowly varying, i.e. $\eta = \eta(Y)$. Substituting (3.4) in (3.3) and keeping it to order ε, the local dispersion relation is obtained from the terms of ε^0 (Whitham 1974):

$$\mathrm{i}\omega(k^2 + l^2) + \mathrm{i}P\eta(Y)k = 0, \quad \text{i.e.} \quad \omega = -\frac{P\eta(Y)k}{k^2 + l^2}, \tag{3.6}$$

where

$$\omega = -\frac{\partial\phi}{\partial T}, \quad k = \frac{\partial\phi}{\partial X}, \quad l = \frac{\partial\phi}{\partial Y} \tag{3.7}$$

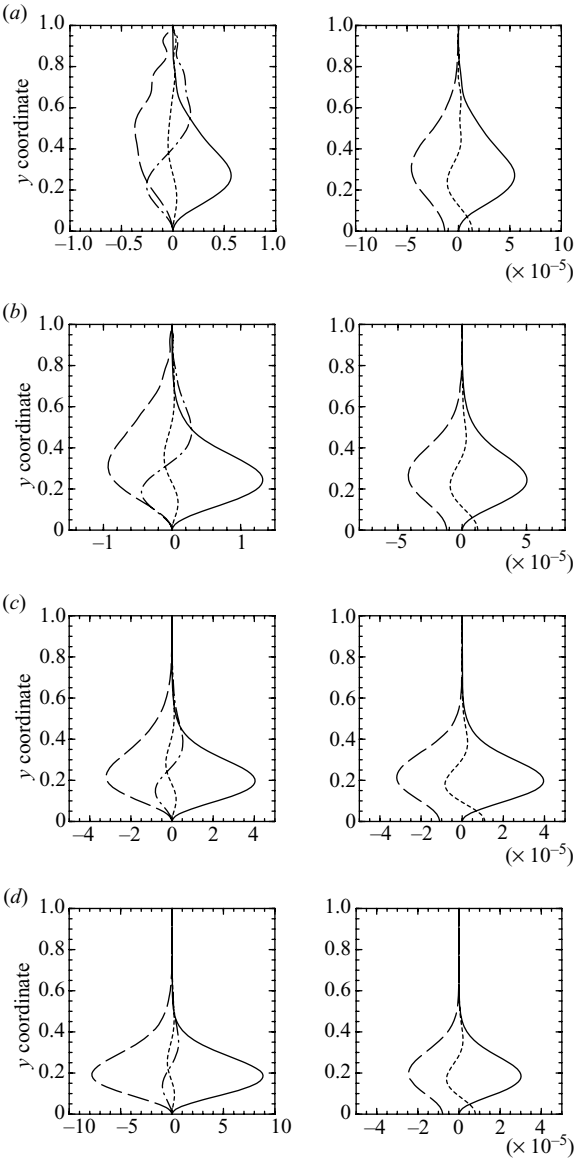

FIGURE 3. Comparison of the terms in the kinetic energy and thermal energy equations for spherical convex boundaries and uniform basic temperature gradient $d\Theta/dy = -1$. The left panel of each figure describes the kinetic energy budget. The solid, broken, dotted and dotted–broken lines denote kinetic energy generation by the buoyancy force, viscous dissipation, convergence of the energy flux by viscosity and convergence of the energy flux by the Rossby waves, respectively. The right panel of each figure describes the thermal energy budget. The solid, broken and dotted lines indicate thermal energy generation by the vertical motion, dissipation by thermal diffusivity and convergence of the energy flux by thermal diffusion, respectively: (*a*) $P = 0.1$, (*b*) $P = 0.2$, (*c*) $P = 0.5$ and (*d*) $P = 1.0$.

are the local frequency and wavenumbers in the x and y directions, respectively. The behaviours of ω, k and l are obtained by the definitions (3.7) and the local dispersion relation (3.6). Since the local dispersion relation is expressed as $\omega = \omega(k, l, Y)$, this

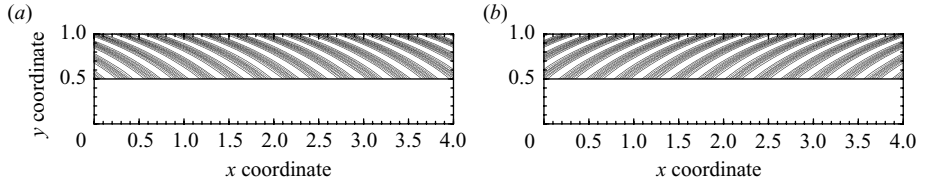

FIGURE 4. Structures of the streamlines for spherical convex boundaries and uniform basic temperature gradient $\mathrm{d}\Theta/\mathrm{d}y = -1$ obtained by the local dispersion relation (3.13). The used parameters are $\omega = -86.0$ and $k = 11.0$, which are those of the critical convection for $P = 0.1$: (*a*) Positive y component of the group velocity (outward, $kl > 0$, $C_{gy} > 0$). (*b*) Negative y component of the group velocity (inward, $kl < 0$, $C_{gy} < 0$).

gives

$$\frac{\partial \omega}{\partial T} = \left(\frac{\partial \omega}{\partial k}\right)_{l,Y} \frac{\partial k}{\partial T} + \left(\frac{\partial \omega}{\partial l}\right)_{k,Y} \frac{\partial l}{\partial T} = -C_{gx}\frac{\partial \omega}{\partial X} - C_{gy}\frac{\partial \omega}{\partial Y}, \tag{3.8}$$

$$\frac{\partial k}{\partial T} = -\frac{\partial \omega}{\partial X} = -\left(\frac{\partial \omega}{\partial k}\right)_{l,Y} \frac{\partial k}{\partial X} - \left(\frac{\partial \omega}{\partial l}\right)_{k,Y} \frac{\partial l}{\partial X} = -C_{gx}\frac{\partial k}{\partial X} - C_{gy}\frac{\partial k}{\partial Y}, \tag{3.9}$$

$$\frac{\partial l}{\partial T} = -\frac{\partial \omega}{\partial Y} = -\left(\frac{\partial \omega}{\partial k}\right)_{l,Y} \frac{\partial k}{\partial Y} - \left(\frac{\partial \omega}{\partial l}\right)_{k,Y} \frac{\partial l}{\partial Y} - \left(\frac{\partial \omega}{\partial Y}\right)_{k,l}$$
$$= -C_{gx}\frac{\partial l}{\partial X} - C_{gy}\frac{\partial l}{\partial Y} - \left(\frac{\partial \omega}{\partial Y}\right)_{k,l}, \tag{3.10}$$

where C_{gx} and C_{gy} are the x and y components of the group velocity:

$$C_{gx} = \left(\frac{\partial \omega}{\partial k}\right)_{l,Y} = \frac{P\eta(Y)(k^2 - l^2)}{(k^2 + l^2)^2}, \quad C_{gy} = \left(\frac{\partial \omega}{\partial l}\right)_{k,Y} = \frac{2P\eta(Y)kl}{(k^2 + l^2)^2}. \tag{3.11}$$

From (3.8) and (3.9), the frequency ω and the wavenumber in the x direction k are found to be conserved because the system is independent of t and x. In contrast, since the coefficient of the topographic β effect η depends on y, the wavenumber in the y direction l varies as the waves propagate in the y direction.

As seen in figure 3, kinetic energy is generated and convective motion is excited in the inner region. Accordingly, we suppose that the Rossby waves with frequency ω and wavenumber k are emitted from $y = 0.5$. As the waves propagate radially and y becomes large, $\eta(Y)$ increases. From the dispersion relation (3.6), the absolute value of l must increase to conserve ω and k. As a result, the wavefront of the Rossby waves inclines and approaches the horizontal surface as they propagate outward, forming a spiral structure.

Expressing this process explicitly, (3.6) is solved for l as

$$l(y) = \pm\sqrt{-\frac{P\eta(y)}{\omega} - k^2}, \tag{3.12}$$

where Y is substituted with y for simplicity. Using $l(y)$, the distribution of the stream function at a given time can be found as follows:

$$\psi(x, y, t) = \hat{\psi}_0 \exp\left\{\mathrm{i}\left(kx + \int_{0.5}^{y} l(y)\mathrm{d}y - \omega t\right)\right\}. \tag{3.13}$$

Figure 4 shows the distributions of the stream function obtained by (3.13) with the frequency and wavenumber of critical convection at $P = 0.1$, showing the cases for

both positive and negative signs in (3.12). The case with $kl > 0$, i.e. a positive group velocity in the y direction, appears to be consistent with the pattern of the critical convection. When the y component of the group velocity is positive, the streamline tilts in the positive y and negative x directions (outward in the prograde direction). In contrast, when the y component of the group velocity is negative, $kl < 0$, and the streamline inclines towards the positive y and positive x directions (outward in the retrograde direction). Thus it can be concluded that the tilting direction of the flow pattern is related to the radial propagation direction of the Rossby waves. We can also explain the spiral structure observed in figure 2 as being formed by the increase of the local radial wavenumber of the Rossby waves propagating from the inner to the outer regions.

The Rossby waves emitted from the inner region are dissipated by the viscous effect during their outward propagation. Because the dissipation rate is $P[k^2 + l(y)^2]$ in unit time, the stream function is evaluated as

$$\psi(x, y, t) = \hat{\psi}_0 \exp\left\{\mathrm{i}\left(kx + \int_{0.5}^{y} l(y)\,\mathrm{d}y - \omega t\right)\right\} \exp\left\{-\int_{0.5}^{y} P(k^2 + l(y)^2)/C_{gy}(y)\,\mathrm{d}y\right\}. \tag{3.14}$$

Figure 5 compares the stream function calculated by (3.14) and that of critical convection obtained numerically for various values of the Prandtl number. The comparison shows that (3.14) well describes the tailing part of the spiral streamline pattern of the critical convection. The radial extent of the streamline obtained by (3.14) is nearly equal to that of the critical convection. It can be seen that at small Prandtl numbers, the propagation distance of the Rossby waves is sufficiently large for a spiral structure to appear because of the small viscous effect. However, it decreases as the Prandtl number increases because of the strong viscous effect, and the flow pattern is localized in the inner region.

3.2. *Concave boundaries*

In this section, the structure of critical convection for the case of concave boundaries is explained by the radial propagation properties of the Rossby waves for the purpose of comparison with the previous section.

Figure 6 shows structures of critical convection for concave boundaries and uniform basic temperature gradient $\mathrm{d}\Theta/\mathrm{d}y = -1$ for various values of the Prandtl number. In contrast to the case of convex boundaries, the flow patterns extend spirally from the outer to the inner regions. The tilting direction of the flow pattern is opposite to that of the convex boundaries and is consistent with asymptotic expansion results for the curvature of the boundaries (Busse 1983*a*, *b*; Busse & Or 1986).

Figure 7 plots each term of the right-hand side of the kinetic energy equation (3.1) and the thermal energy equation (3.2) for the critical convection shown in figure 6. It can be seen that kinetic energy is generated by the buoyancy force in the outer-half region. When the Prandtl number is large, both kinetic and thermal energies are dissipated by viscosity and thermal diffusivity in the same energy-generating region. As the Prandtl number decreases, the region of viscous dissipation extends inward, while the generation of kinetic and thermal energies and the dissipation of thermal energy still occur inside the outer-half region. At the same time, the ratio of kinetic energy flux convergence by the Rossby waves increases. The convergence is negative in the outer region and positive in the inner region. This means that the Rossby waves are excited in the outer region, propagate inward in association with kinetic energy

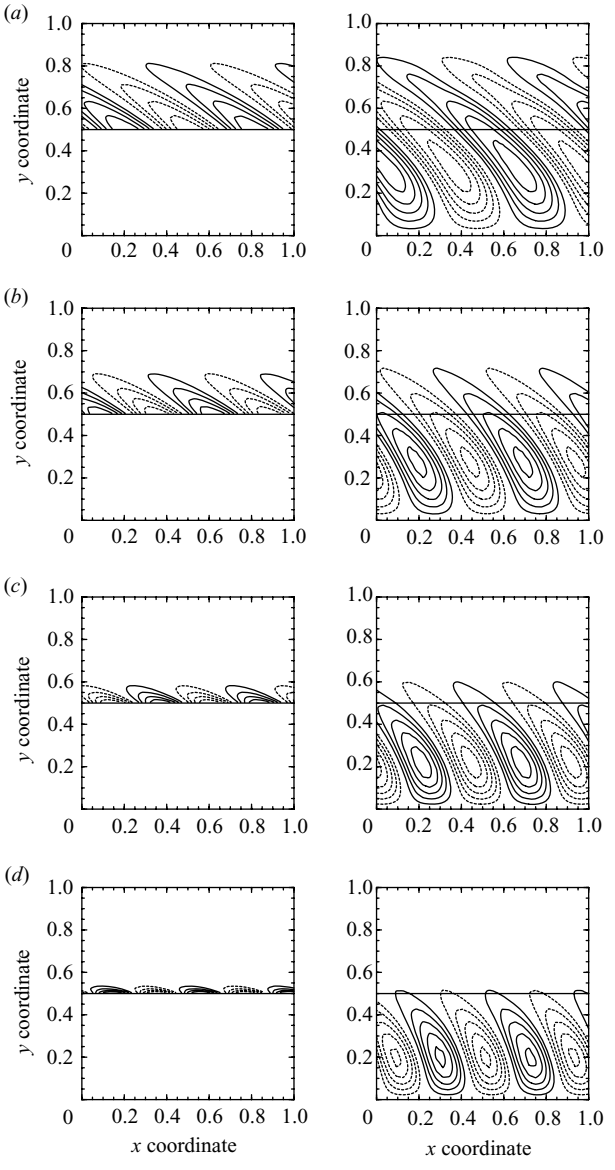

FIGURE 5. Comparison of the patterns of the stream function obtained by the local dispersion relation (3.14) (left panels) and those of the critical convection calculated numerically (right panels) for the spherical convex boundaries and the uniform basic temperature gradient $\mathrm{d}\Theta/\mathrm{d}y = -1$. The structures above the horizontal lines $y = 0.5$ should be compared: (*a*) $P = 0.1$, $\omega = -86.2$, $k = 10.2$; (*b*) $P = 0.2$, $\omega = -181.8$, $k = 12.6$; (*c*) $P = 0.5$, $\omega = -245.1$, $k = 13.3$; (*d*) $P = 1.0$, $\omega = -344.3$, $k = 14.9$.

and are dissipated in the inner region. It can also be observed that the dynamic factors dominate energy budget in the inner-half region, and the thermal factors become less important as the Prandtl number is decreased.

Since kinetic energy is generated and convective motion is excited in the outer-half region, we suppose that the Rossby waves with frequency ω and wavenumber k are emitted from $y = 0.5$. As the waves propagate radially and y becomes small, $\eta(Y)$

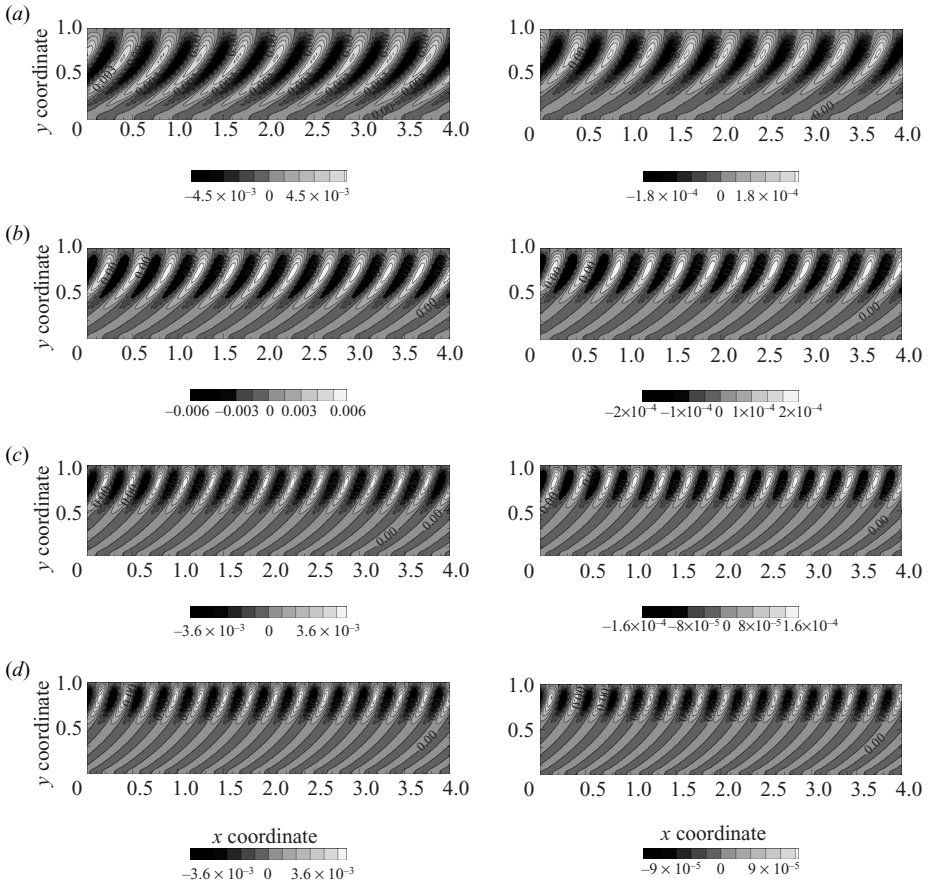

FIGURE 6. Structures of critical convection for concave boundaries (compare with figure 2 for convex boundaries) and uniform basic temperature gradient $\mathrm{d}\Theta/\mathrm{d}y = -1$ for various values of the Prandtl number: (*a*) $P = 0.1$, (*b*) $P = 0.2$, (*c*) $P = 0.5$ and (*d*) $P = 1.0$. The left and right panels show the stream function and the temperature disturbance, respectively.

increases. Then, the wavenumber in the y direction $l(y)$ varies according to (3.12), and the absolute value of l increases to conserve ω and k. As a result, the wavefront of the Rossby waves inclines and approaches the horizontal surface as they propagate inward, and a spiral structure is formed. The explicit expression of the distribution of the stream function at a given time is as follows:

$$\psi(x, y, t) = \hat{\psi}_0 \exp\left\{ \mathrm{i} \left(kx + \int_y^{0.5} l(y)\, \mathrm{d}y - \omega t \right) \right\}. \tag{3.15}$$

Figure 8 shows the distributions of the stream function obtained by (3.15) with the frequency and wavenumber of critical convection at $P = 0.1$. Similar to the previous section, the cases with positive and negative signs in (3.12) are shown. The case with $kl < 0$, i.e. negative group velocity in the y direction, is consistent with the pattern of the critical convection.

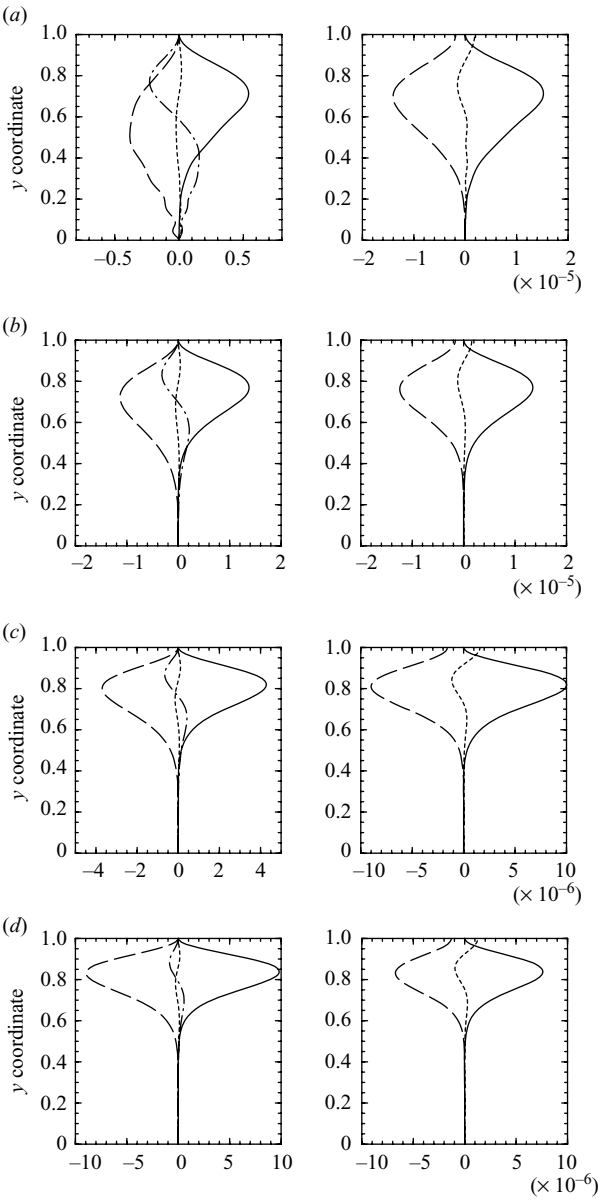

FIGURE 7. The same as figure 3 but for the concave boundaries and the uniform basic temperature gradient $\mathrm{d}\Theta/\mathrm{d}y = -1$: (*a*) $P = 0.1$, (*b*) $P = 0.2$, (*c*) $P = 0.5$ and (*d*) $P = 1.0$.

Moreover, evaluating the effect of viscous dissipation, the distribution of the stream function becomes

$$\psi(x, y, t) = \hat{\psi}_0 \exp\left\{\mathrm{i}\left(kx + \int_y^{0.5} l(y)\,\mathrm{d}y - \omega t\right)\right\} \exp\left\{-\int_y^{0.5} P(k^2 + l(y)^2)/C_{gy}(y)\,\mathrm{d}y\right\}. \tag{3.16}$$

Figure 9 compares the stream function calculated by (3.16) and that of critical convection obtained numerically for various values of the Prandtl number. The comparison shows that (3.16) well describes the structure of the stream function of

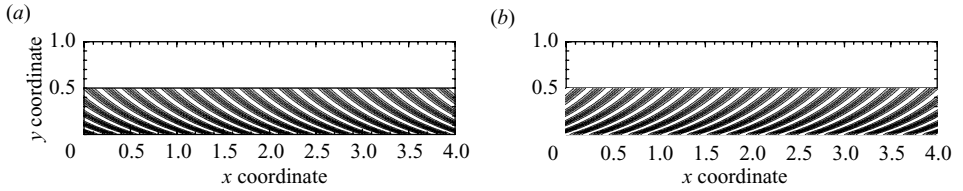

FIGURE 8. Structures of the streamlines for concave boundaries (compare with figure 4 for convex boundaries) and uniform basic temperature gradient $\mathrm{d}\Theta/\mathrm{d}y = -1$ obtained by the local dispersion relation (3.13). The parameters are $\omega = -208.5$, $k = 14.9$, which are those of the critical convection for $P = 0.1$: (*a*) Positive y component of the group velocity (outward, $kl > 0$, $C_{gy} > 0$); (*b*) Negative y component of the group velocity (inward, $kl < 0$, $C_{gy} < 0$).

critical convection. Similar to the case of convex boundaries, it is observed that the propagation distance of the Rossby waves decreases as the Prandtl number increases and the viscous effect becomes strong. The radial extent of the streamline obtained by (3.16) is nearly equal to that of the critical convection.

3.3. *Inverse tilting direction*

We have seen in the previous sections that the tilting direction of the flow pattern is determined by the radial propagation direction of the Rossby waves. The results imply that the curvature of the boundaries is the only factor determining the region where the convective motion and the Rossby waves are excited. In order to confirm these statements, this section presents two artificial but instructive solutions with the tilting direction of the flow pattern inverse to that expected from the curvature of the boundaries.

The first solution is of the case in which the boundaries are convex and the thermally unstable region is confined near the outer boundary:

$$\frac{\mathrm{d}\Theta}{\mathrm{d}y} = -\exp\left(-\frac{(y-1)^2}{y_b^2}\right), \tag{3.17}$$

where y_b is the typical width of the unstable region. Figure 10(*a*) shows the distributions of the stream function and temperature disturbance for $y_b = 0.01$ and $P = 0.1$. Although the tilting direction of the temperature disturbance contours is inward in the retrograde direction, the flow pattern tilts inward in the prograde direction. This is the inverse of what is expected, considering the curvature of the boundaries. In this case, since only the region near the outer boundary is unstable, the propagation direction of the emitted Rossby waves is forced to be inward. Therefore, kl is negative and the flow pattern tilts in the positive x and positive y directions. The energy budget of the critical convection is shown in figure 11(*a*). The convergence of the energy flux by the Rossby waves shows that the Rossby waves generated near the outer boundary propagate and transport kinetic energy inward.

The second solution is of the case in which the boundaries are concave and the thermally unstable region is confined near the inner boundary:

$$\frac{\mathrm{d}\Theta}{\mathrm{d}y} = -\exp\left(-\frac{y^2}{y_b^2}\right). \tag{3.18}$$

Figure 10(*b*) shows the distributions of the stream function and temperature disturbance for $y_b = 0.01$ and $P = 0.1$. The tilting direction of the flow pattern is

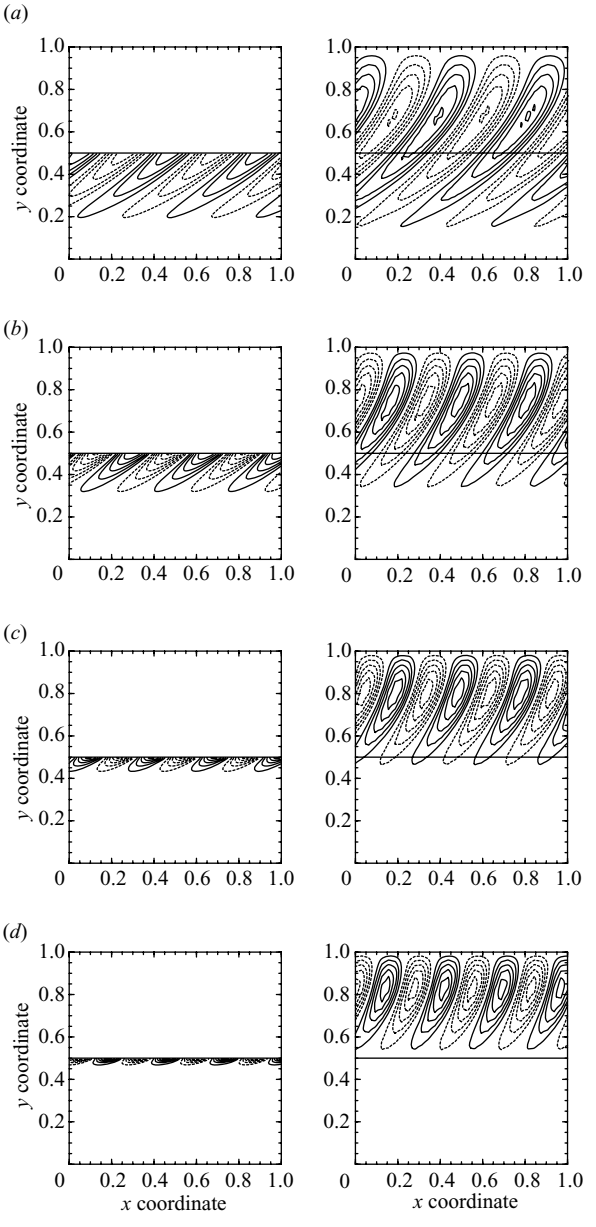

FIGURE 9. Comparison of the patterns of the stream function obtained by the local dispersion relation (3.14) (left panels) and those of the critical convection calculated numerically (right panels) for concave boundaries (compare with figure 5 for convex boundaries) and uniform basic temperature gradient $\mathrm{d}\Theta/\mathrm{d}y = -1$. The structures below the thick horizontal lines should be compared: (*a*) $P = 0.1$, $\omega = -208.5$, $k = 14.9$; (*b*) $P = 0.2$, $\omega = -420.1$, $k = 19.6$; (*c*) $P = 0.5$, $\omega = -566.6$, $k = 21.2$; (*d*) $P = 1.0$, $\omega = -799.0$, $k = 22.8$.

outward in the prograde direction, which is the inverse of what is expected, considering the curvature of the boundaries. In this case, since the propagation direction of the emitted Rossby waves is forced to be outward because of the inner boundary, kl is positive, and the flow pattern tilts in the negative x and positive y directions. The kinetic energy budget presented in figure 11(*b*) shows that the convergence of the

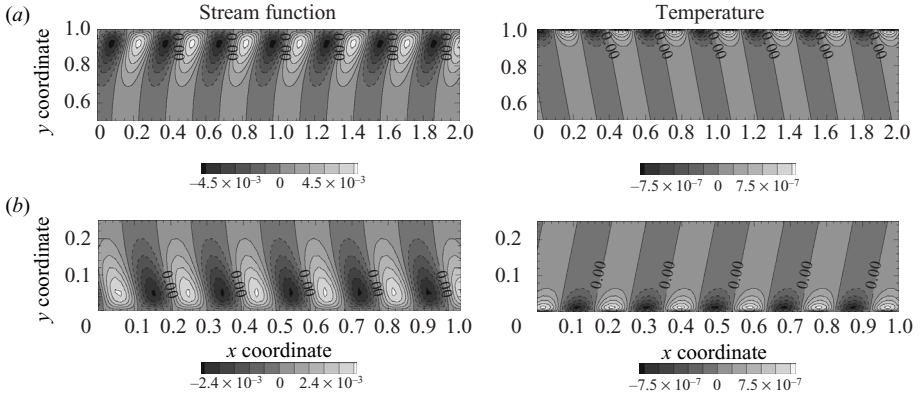

FIGURE 10. Structures of critical convection whose flow patterns are tilted in a direction inverse to that expected from the curvature of the boundaries. (*a*) Convex boundaries and basic temperature gradient given by (3.17) ($y_b = 0.01$, $P = 0.1$). (*b*) Concave boundaries and basic temperature gradient given by (3.18) ($y_b = 0.01$, $P = 0.1$). The left and right panels show the stream function and the temperature disturbance, respectively.

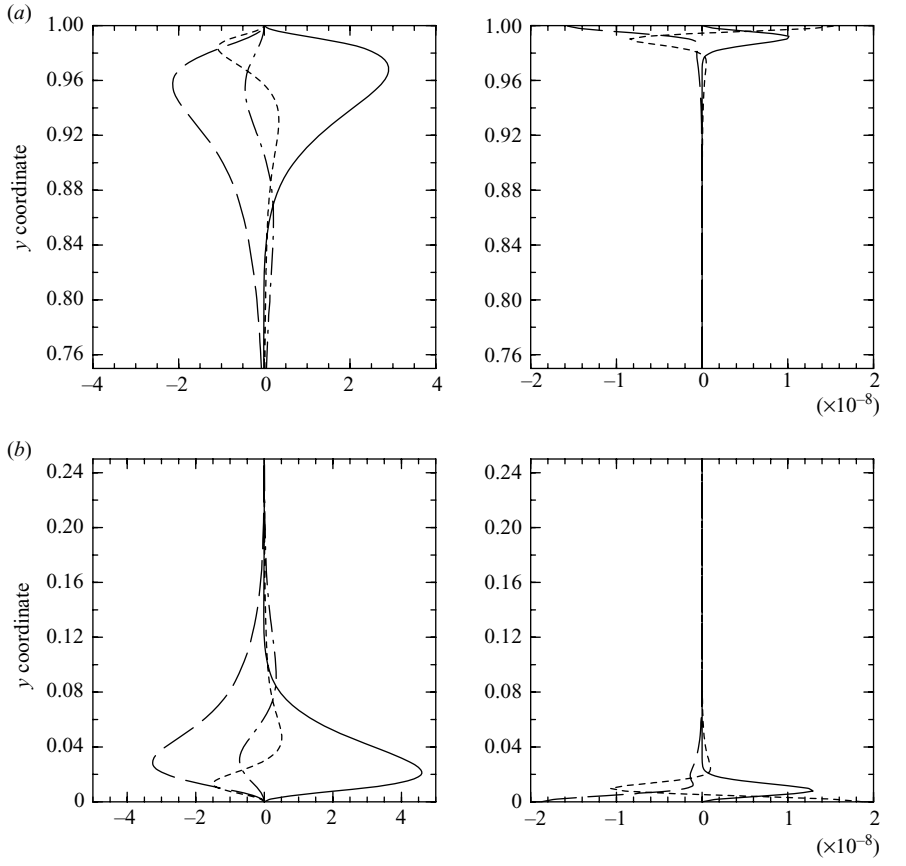

FIGURE 11. The same as figures 3 and 7 but for a basic temperature gradient confined near the boundaries: (*a*) convex spherical boundaries ($y_b = 0.01$, $P = 0.1$); (*b*) concave boundaries ($y_b = 0.01$, $P = 0.1$).

energy flux by the Rossby waves indicates outward propagation of the Rossby waves from near the inner boundary.

4. Summary

We have interpreted the characteristics of two-dimensional spiral convection in a rotating annulus with convex and concave boundaries containing the fluid in the direction of the rotation axis through the radial propagation properties of the Rossby waves. An energy budget analysis, which is usually performed for hydrodynamic instability problems, had not been carried out for the spiral convection problem so far. Thus the result of the budget analysis gives us a new finding on the spiralling convection: the spiralling convection has a structure such that kinetic energy is generated in the region with a weak topographic β effect, dynamically transferred to the region with a strong β effect and dissipated there by viscosity. On the basis of this result, the theory of the Rossby wave dynamics is applied to the tailing part of the spiral structure, and it is shown that the spiral structure is well explained by the simple dispersion relation of the traditional Rossby waves.

An important conclusion is that the tilting direction of the spiral-flow pattern is determined not by the curvature of the boundaries but by the radial propagation direction of the Rossby waves excited by thermal convection. The geometry of the boundaries in the direction of the rotating axis is the only factor determining the place of occurrence of thermal convection. We have presented examples in which the tilting direction is inverse to that expected from the curvature. In these cases, the kinetic energy budget analysis confirms that the tilting direction of the flow pattern is determined by the propagation direction of the Rossby waves.

A further conclusion is that the spiral convective structure is well described by the radial propagation properties of the Rossby waves. In the case of convex spherical boundaries, thermal convection tends to occur in the inner region where the inclination of the boundaries is weak. The Rossby waves excited by convection in the inner region propagate outward and dissipate by viscosity. As the Rossby waves propagate outward, the radial local wavenumber increases and a spiral structure is formed. For concave boundaries, the inclination of the boundaries is weak in the outer region, where thermal convection tends to occur. The Rossby waves excited there propagate inward and dissipate in the inner region. As a result, a spiral pattern with a tilting direction inverse to that of the convex boundary case is formed. The flow patterns calculated by the dispersion relation are consistent with those of the critical convection obtained numerically. The kinetic energy budget analysis also confirms the geometry of the propagation of the Rossby waves, which is important for forming the spiral structure. The reason for the outward-prograde tilting of the streamlines in the case of convex boundaries is the increase of the radial wavenumber in the outer region as a result of conservation of the phase speed of the Rossby waves; it is not because the propagation speed in the longitudinal direction is faster in the outer region than in the inner region (Busse 2002; Vasavada & Showman 2005).

For convex spherical boundaries, the structure of the critical convection has characteristics similar to that of thermal convection in rapidly rotating spherical shells. When the Prandtl number is large, radially confined Taylor-column-type vortices appear in the inner region. As the Prandtl number decreases, they extend outward and form a spiral structure. Therefore, it is expected that two-dimensional convection in a rotating annulus with the properties of the Rossby waves can be applied to convection in rapidly rotating spheres and spherical shells. Convective

motion in rapidly rotating spheres and spherical shells without internal heating tends to occur near the axial cylindrical surface tangent to the inner sphere, where the inclination of the boundary is weak (Dormy *et al.* 2003). Alternatively, for uniform internal heating, convection in rapidly rotating spheres and spherical shells tends to occur in the middle of the sphere because of the competition between the inhibitory effect of the tilting boundaries on the occurrence of thermal convection and the extent of thermal instability, which increases outward (Busse 1970). When the Prandtl number is small, the viscous effect is weak and the Rossby waves excited by thermal convection in the inner or the middle region can propagate outward. This constitutes spiralling-columnar convection. In contrast, when the Prandtl number is large, the viscous effect is strong and the Rossby waves cannot propagate outward and fluid motion is confined in the inner or middle region. This forms Taylor-column-type convection.

The generation of mean zonal flows excited by spiralling convection is usually explained by the Reynolds stress accompanying the tilting of the flow pattern. In the case of convex spherical boundaries, the Reynolds stress $\overline{v_x v_y}$, which is produced by the correlation of the x and y components of the velocity v_x and v_y, is negative, and momentum in the negative x direction (prograde) is transported outward and prograde mean zonal flow is generated in the outer region. However, this mean zonal flow generation can also be explained by the properties of the Rossby waves. Since the phase speed c in the x direction of the topographic Rossby waves is negative (prograde), the momentum of the Rossby waves E/c is in the same direction, where E is the energy of the Rossby waves. As seen in § 3.1, since the Rossby waves are emitted from the inner region, negative momentum is lost there. As a result, positive momentum is left and retrograde mean zonal flow is generated. Alternatively, in the outer region, the Rossby waves are injected and dissipated. Therefore, negative momentum accumulates there and prograde mean zonal flow is generated.

It should be noted that the above argument holds because of the separation of the thermal factors in the outer region: the thermal effects concentrate in the inner region and only the dynamical factors are sufficient for consideration of fluid motion in the outer region; for example, in the case of a constant coefficient of the topographic β effect and uniform unstable stratification, the convection cells do not tilt and the second-order mean zonal flow is not induced by thermal convection (Busse & Or 1986), whereas the momentum of the dynamic Rossby waves seems to remain finite. Because the thermal effects spread over the whole domain in this case, conservation of potential vorticity is broken, and then, discussion in terms of the second-order momentum of the Rossby waves for this example becomes inappropriate.

Jones, Soward & Mussa (2000, hereafter JSM) used the WKBJ (Wentgel–Krasfamers–Brillouin–Jeffreys) method on the complex radial coordinate to determine the structure and critical parameters of convection in a rotating sphere (Jones *et al.* 2000), while in this study the spiral structure is examined by using the traditional Rossby waves on the real radial coordinate, thanks to cutting out the tailing part of the spiral convection. The approach of JSM is mathematically clear and straightforward in obtaining the critical mode of convection. However, mathematical completeness does not always bring physical understanding. The approach of this paper is expected to complement it. The explanation of spiral structure using the simple dispersion relation presented in this paper would clarify the physical structure of the group velocity and spatial gradients of the frequency embedded in the analysis of JSM; for example reflection of the spatial gradients of the frequency on the spiral convection is interpreted by the terms of the Rossby wave dynamics as the radial wavenumber

variation to conserve the frequency. Furthermore, it is shown that the direction of the tilting of the spiral structure is connected with the sign of the group velocity of the Rossby waves, which is difficult to grasp at a glance from the analysis of JSM.

Certainly, there are several points left to be unravelled; for example the frequency gradient condition at the critical point is not included in the discussions of this paper. In the asymptotic theory of JSM, the condition of vanishing of group velocity at the critical point leads to the flow structure around the convection centre and the critical values of the parameters. On the other hand, our discussion deals with the spiral structure far from the convection centre, and critical values of the Rayleigh number and azimuthal wavenumber are given by the numerical results. Nevertheless, the value of the paper, i.e. a simple description of the tailing part of the spiral structure by the traditional Rossby wave dynamics, is not diminished. Generally, since the Rossby wave originates from the conservation of potential vorticity, which is not a term restricted to meteorology and oceanography but a general concept of fluid dynamics, describing phenomena by the Rossby waves and explaining them through the concept of potential vorticity is meaningful for researchers not only in meteorology and oceanography but also in more extensive surrounding fields such as fluid dynamics and physics (e.g. Baldwin *et al.* 2007). For example Yano *et al.* (2005) perform numerical experiments on columnar two-dimensional free-decaying turbulence in a rotating sphere and interpret their results through the concept of potential vorticity. Following this context, the analyses presented in this paper would help the further understanding of the spiral convection.

The author thanks Professor Y.-Y. Hayashi and Professor M. Yamada for their helpful discussions and encouragements. He is also grateful to three anonymous reviewers for their useful comments. For the calculation of the critical modes of convection, the library for spectral transform 'ISPACK' (http://www.gfd-dennou.org/library/ispack/) and its Fortran90 wrapper library 'SPMODEL library' (Takehiro *et al.* 2006) were used. The eigenvalue problems were solved with the subroutine 'LAPACK' (ftp://ftp.netlib.org/lapack/). The products of the Dennou Ruby project (http://www.gfd-dennou.org/library/ruby/) were used for drawing the figures.

REFERENCES

Aurnou, J. M. & Olson, P. L. 2001 Strong zonal winds from thermal convection in a rotating spherical shell. *Geophys. Res. Lett.* **28**, 2557–2559.

Baldwin, M. P., Rhines, P. B., Huang, H.-P. & McIntyre, M. E. 2007 The jet-stream conundrum. *Science* **315**, 467–468.

Busse, F. H. 1970 Thermal instabilities in rapidly rotating systems. *J. Fluid Mech.* **44**, 441–460.

Busse, F. H. 1983*a* Convection-driven zonal flows in the major planets. *PAGEOPH* **121**, 375–390.

Busse, F. H. 1983*b* A model of mean zonal flows in the major planets. *Geophys. Astrophys. Fluid Dyn.* **23**, 153–174.

Busse, F. H. 1986 Asymptotic theory of convection in a rotating, cylindrical annulus. *J. Fluid Mech.* **173**, 545–556.

Busse, F. H. 2002 Convective flows in rapidly rotating spheres and their dynamo action. *Phys. Fluids* **14**, 1301–1314.

Busse, F. H. & Hood, L. L. 1982 Differential rotation driven by convection in a rapidly rotating annulus. *Geophys. Astrophys. Fluid Dyn.* **21**, 59–74

Busse, F. H. & Or, A. C. 1986 Convection in a rotating cylindrical annulus: thermal Rossby waves. *J. Fluid Mech.* **166**, 173–187.

Christensen, U. R. 2001 Zonal flow driven by deep convection in the major planets. *Geophys. Res. Lett*. **28**, 2553–2556.

Dormy, E., Soward, A. M., Jones, C. A., Jault, D. & Cardin, P. 2003 The onset of thermal convection in rotating spherical shells. *J. Fluid Mech.* **501**, 43–70.

Jones, C. A., Soward, A. M. & Mussa, A. I. 2000 The onset of thermal convection in a rapidly rotating sphere. *J. Fluid Mech.* **405**, 157–179.

Lin, R.-Q. 1990 Double column instabilities in the barotropic annulus. *Geophys. Astrophys. Fluid Dyn.* **54**, 161–188.

Or, A. C. & Busse, F. H. 1987 Convection in a rotating cylindrical annulus. Part 2. Transitions to asymmetric and vacillating flow. *J. Fluid Mech.* **174**, 313–326.

Pedlosky, J. 1987 *Geophysical Fluid Dynamics*. Springer.

Plaut, E. & Busse, F. H. 2005 Multicellular convection in rotating annuli. *J. Fluid Mech.* **528**, 119–133.

Schnaubelt, M. & Busse, F. H. 1992 Convection in a rotating cylindrical annulus. Part 3. Vacillating and spatially modulated flows. *J. Fluid Mech.* **245**, 155–173.

Takehiro, S. & Hayashi, Y.-Y. 1999 Mean zonal flows excited by critical thermal convection in rotating spherical shells. *Geophys. Astrophys. Fluid Dyn.* **90**, 43–77.

Takehiro, S., Ishiwatari, M., Nakajima, K. & Hayashi, Y.-Y. 2002 Linear stability of thermal convection in rotating systems with fixed heat flux boundaries. *Geophys. Astrophys. Fluid Dyn.* **96**, 439–459.

Takehiro, S., Odaka, M., Ishioka, K., Ishiwatari, M., Hayashi, Y.-Y. & SPMODEL Development Group. 2006 A series of hierarchical spectral models for geophysical fluid dynamics. *Nagare Multimedia 2006*, http://www.nagare.or.jp/mm/2006/spmodel/.

Vasavada, A. R. & Showman, A. P. 2005 Jovian atmospheric dynamics: an update after Galileo and Cassini. *Rep. Prog. Phys.* **68**, 1935–1996.

Whitham, G. B. 1974 *Linear and Nonlinear Waves*. John Wiley & Sons.

Yano, J.-I. 1992 Asymptotic theory of thermal convection in rapidly rotating systems. *J. Fluid Mech.* **243**, 103–131.

Yano, J.-I., Talagrand, O. & Drossart, P. 2005 Deep two-dimensional turbulence: an idealized model for atmospheric jets. *Geophys. Astrophys. Fluid Dyn.* **99**, 137–150.

Zhang, K. 1992 Spiralling columnar convection in rapidly rotating spherical fluid shells. *J. Fluid Mech.* **236**, 535–556.

Zhang, K.-K. & Busse, F. H. 1987 On the onset of convection in rotating spherical shells. *Geophys. Astrophys. Fluid Dyn.* **39**, 119–147.